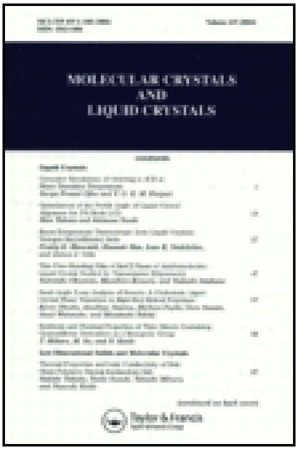

Molecular Crystals and Liquid Crystals Science and Technology. Section A. Molecular Crystals and Liquid Crystals

Publication details, including instructions for authors and subscription information:
http://www.tandfonline.com/loi/gmcl19

# Optimization of Holographic PDLC for Binary Monomers

Byung Kyu Kim [a] , Young Chan Jeon [a] & Jae Chang Kim [b]

[a] Dept. of Polymer Science and Engineering, Pusan National University, Pusan, 609-735, Korea

[b] Dept. of Electronic Engineering, Pusan National University, Pusan, 609-735, Korea

Version of record first published: 24 Sep 2006

To cite this article: Byung Kyu Kim, Young Chan Jeon & Jae Chang Kim (1999): Optimization of Holographic PDLC for Binary Monomers, Molecular Crystals and Liquid Crystals Science and Technology. Section A. Molecular Crystals and Liquid Crystals, 326:1, 319-331

To link to this article: http://dx.doi.org/10.1080/10587259908025423

*Mol. Cryst. Liq. Cryst.*, Vol. 326, pp. 319–331
Reprints available directly from the publisher
Photocopying permitted by license only

# Optimization of Holographic PDLC for Binary Monomers

BYUNG KYU KIM[a],*, YOUNG CHAN JEON[a] and JAE CHANG KIM[b]

[a] *Dept. of Polymer Science and Engineering,*
[b] *Dept. of Electronic Engineering, Pusan National University, Pusan 609-735, Korea*

*(Received 15 September 1998; In final form 10 November 1998)*

Reflective holographic polymer dispersed liquid crystals (HPDLC) have been fabricated by irradiating Ar-ion laser of various intensities on LC/acrylate monomer mixtures of various compositions sandwiched between two ITO coated glass plates. Polarized optical micrography (POM), scanning electron microscopy (SEM) images of the gratings and UV-visible spectra of the films have been obtained and reflection efficiency-irradiation intensity-monomer ratio relationships have been obtained.

*Keywords:* Holography; polymer dispersed liquid crystal; UV-visible; POM; SEM

## INTRODUCTION

Polymer dispersed liquid crystal (PDLC) is a thin composite film composed of micron-sized droplets of low-molecular weight Liquid crystal (LC) of typically positive dielectric anisotropy dispersed in an optically isotropic polymer matrix [1–5]. PDLC has potentials for a variety of electrooptic applications ranging from direct driven smart window to active matrix driven information displays. A number of important reviews regarding the methods of preparation, materials, modes of operation, device applications, *etc.*, have become available [6–10]. Recently, a monograph which is totally devoted to LC dispersions has also appeared [11].

The conventional PDLC makes use of the light scatterings in the absence of external field, and light transmittance in the presence of external field.

---

*Corresponding author. Tel.: +82 51 510 2406, Fax: +82 51 514 1726.

Therefore it is imperative that the droplet size be order of micrometers with certain size distribution so that the broad spectrum of visible-range lights can scatter at the interfaces to make the film white [12–15].

Regarding the type of polymeric materials used for matrix or host for LC, UV-curable acrylates have most often been encountered due to their high optical clarity and diverse freedom of property variations [6–20]. In UV-curable system, LCs are mixed with prepolymer (polymer precursor), reactive diluents, and photoinitiator to form a single phase. Typical reactive diluents are mono-, di-, and trifunctional acrylates and these are added to reduce the prepolymer viscosity and to build up the molecular weight of host polymer by chain extension (monoacrylate) and crosslinking (multifunctional acrylates). The extent of crosslinking and rate of reaction largely depend on the average functionality of monomer mixture.

Recently volume holography technique has been applied to the PDLC and fabricated controlled architectures of phase separated LC domains [21–27]. This type of PDLC is called holographic polymer dispersed liquid crystal (HPDLC) in literature [26]. This new technique is based on the polymerization induced phase separation (PIPS) and Bragg's law (Eq. 1) given below:

$$\Lambda = \frac{\lambda}{2\sin\theta} \tag{1}$$

where $\lambda$ is the wavelength of light, $\Lambda$ is the grating spacing, and $2\theta$ is the inter beam angle outside the film.

Simple methods of optical alignment to control the grating spacing using a single wavelength laser are available [27]. The interference fringes of laser irradiation onto a LC/monomer mixture set up a periodic intensity profile, which in turn causes a periodic spatial modulation of polymerization kinetics [21]. LC molecules are phase separated with the progress of polymerization reaction, and diffused out of the polymer lamellae to form LC domains, which ideally are also macroscopically lamellae. Consequently, periodic lamellae of LC domains separated by polymer walls are fabricated. This periodic structures of multilayers have very promising optical properties since a specific component of the incident light is reflected by the LC droplets due to the difference in the refractive indices of the polymer and LC. For example, grating spacing of 488 nm reflects blue, 514 nm reflects green, and 633 nm reflects red. A full color display can ideally be constructed by stacking three different elements, each reflecting one primary color, respectively [27]. Upon applying the electric field, the refractive index of LC matches that of polymer and all components of the incident light pass through the film and the film becomes transparent.

In HPDLC unwanted light scatterings should be minimized since this device operates based on light reflection rather than the light scatterings in conventional PDLC, and the reflection efficiency is electrically controlled *via* the refractive index of LC molecules [21, 27]. To minimize the scatterings, one should be able to control the LC domain significantly smaller than the wavelength of visible light, *viz.*, nanometer-sized domains are essential.

The domain size in PIPS is relevant to the rates of polymerization and phase separation. In PIPS phase separation occurs with the progress of polymerization due to the unfavorable increase in Gibbs free energy of mixing ($\Delta G_{\mathrm{mix}}$) owing to the decrease in the entropy of mixing ($\Delta S_{\mathrm{mix}}$) since progressively smaller number of molecules become involved:

$$\Delta G_{\mathrm{mix}} = \Delta H_{\mathrm{mix}} - T\Delta S_{\mathrm{mix}} \tag{2}$$

where $T$ is the absolute temperature.

Phase separation phenomenon is a rate process where such transport property as diffusivity takes an important role in determining the rate of phase separation. Diffusion of low molecular species such as low molecular weight LC through polymer greatly depends on the viscosity of polymer which, on the other hand depends on the degree of polymerization.

Since the phase separation is driven by polymerization reaction, rate of polymerization which is given below for photoinitiated radical mechanism largely governs the phase separation and hence the domain size.

$$R_i = 2\phi\varepsilon I_o[A]b \tag{3}$$

$$R_p = K_p[M]\left(\frac{\phi\varepsilon I_o[A]v}{K_t}\right)^{1/2} \tag{4}$$

Detailed procedure to obtain the initiation rate ($R_i$) and polymerization rate ($R_p$) are available elsewhere [28, 29]. In these equations $\phi$, $\varepsilon$, $I_o$, and $b$ are respectively initiation efficiency, molar absorptivity, incident light intensity, and sample thickness. $[M]$ and $[A]$ are the concentration of monomer and species which undergoes photoexcitation, $k_p$ and $k_t$ are rate constant for propagation and termination reactions, respectively. Irradiation power intensity, concentrations of photoinitiator and monomers contribute to $R_p$. However, the former two contribute more to the $R_i(\propto I_o, [A])$ than the $R_p(\propto \sqrt{I_o}, \sqrt{[A]})$ so molecular weight build up is not necessarily obtained with high $I_o$ and $[A]$. Monomer concentration ($[M]$) *viz.*, monomer functionality contributes solely to the $R_p(\propto[M])$, and effectively to the molecular weight build up or network formation of host polymer. With rapid enough rate of polymerization, phase separation can not follow polymerization kinetics since time scale for polymerization is smaller and that of phase separation becomes larger due to the slower diffusion of LC molecules in highly viscous media. So, monomers to be used for HPDLC should have higher functionality than those for conventional PDLC.

We optimized holographic PDLC device to obtain high reflection efficiency. Binary monomer mixtures with different compositions have been irradiated with Ar-ion (488 nm) laser at various intensities. Polarized optical micrograph and scanning electron microscopy images of the gratings were obtained to visualize the holographic gratings. UV-visible spectra were taken to obtain the architectured reflections from gratings. Three dimensional plots of reflection efficiency-laser intensity-monomer composition are presented showing contours for maximum reflections.

## EXPERIMENTAL

### Materials

The LC used in our experiments was E7 (BL001, Merck), a eutectic mixture of four cyanobiphenyl and cyanoterphenyl mixture with $T_{KN} = -10°C$, $T_{NI} = 60.5°C$, $\varepsilon_{\|} = 19.0$, and $\varepsilon_{\perp} = 4.2$. Two types of photopolymerizable monomers (Fig. 1), *viz.*, dipentaerythrol hydroxy penta acrylate(DPHPA,

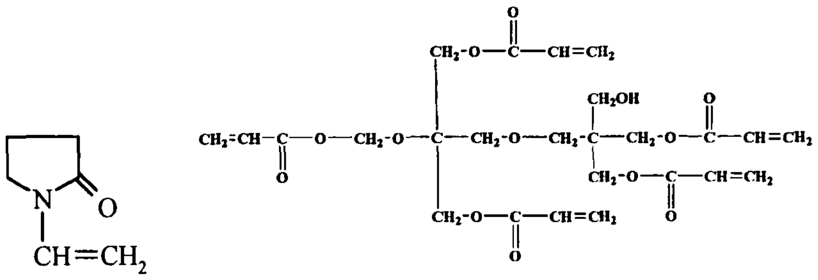

NVP DPHPA

FIGURE 1 Chemical structures of photopolymerizable monomers.

functionality($f$) = 5), and N-vinylpyrrollidone (NVP, $f = 1$) have, in various combinations, been used to prepare the host polymers upon laser irradiation.

Multifunctional monomers *viz.*, DPHPA has much higher reactivity as well as high viscosity due to their high molecular weight, and provide the polymers with extensive crosslinkings, whereas monofunctional NVP simply extends the chains at much lower rate. However, the use of monofunctional monomers is oftentimes essential to reduce the viscosity of LC/monomer mixture and makes the starting mixture homogeneous. Otherwise, PIPS starts with heterogeneous reaction mixture and the morphology of the composite film becomes out of control.

Rose bengal is known as an ideal initiator for holographic recording with Ar-ion laser as it displays a broad absorption spectrum with a peak molar extension coefficient of $\sim 10^4 M^{-1} cm^{-1}$ at about 490 nm [21]. To this, a millimolar amount of N-phenylgycine (NPG) as coinitiator was added. In this experiment $3 \times 10^{-6}$ M of RB and $1.2 \times 10^{-4}$ M of NPG were used.

## Formulations

Holograms were formulated with different monomer and film compositions which were irradiated at various laser intensities. Basically, binary (DPHPA/NVP) systems at a fixed film composition (LC/monomer = 35/65 by weight) were considered and their formulations are given in Table I. The effects of monomer ratio as a function of irradiation intensity were studied.

## Gratings

The holographic recording system is schematically shown in Figure 2. Ar-ion laser ($\lambda = 488$ nm) was used as light source. Beam passes through a spatial filter, beam expander, and is splitted into two with identical intensity. These two beams are subsequently passed through collimator and only the

TABLE I Formulation to prepare HPDLC from DPHPA and NVP

| *Monomer Ratio (DPHPA : NVP)* | *LC : Monomer* | *Rose Bengal (wt%)* | *NPG (wt%)* | *Intensity (mW/cm²)* |
|---|---|---|---|---|
| 4 : 1 | 35 : 65 | 0.3 | 1.8 | 20 ~ 200 |
| 4.5 : 1 | | | | |
| 5 : 1 | | | | |
| 5.5 : 1 | | | | |
| 6 : 1 | | | | |
| 7 : 1 | | | | |

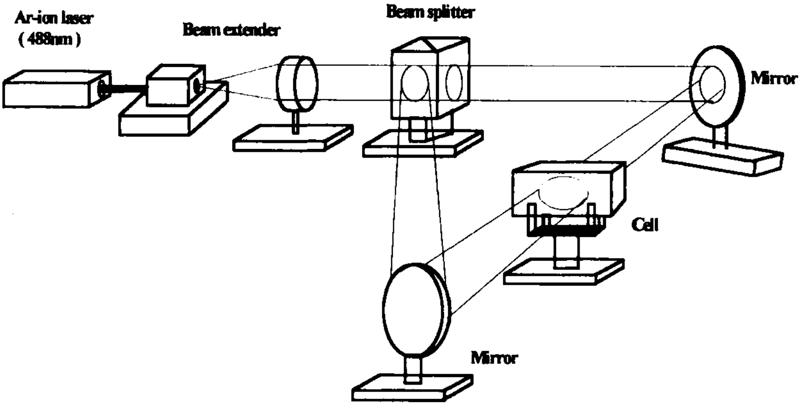

FIGURE 2 Experimental setup for holographic PDLC.

central portions were reflected from the mirrors and impinged normally on the cell from the opposite sides. Cell was constructed by sandwiching the LC/monomer mixture between two indium tin-oxide (ITO) coated glass plates, with a gap of 15 μm adjusted by bead spacer [30]. Interference of two beams established the periodic interference pattern according to Bragg's law which is approximately 488 nm for our case. The laser intensity was varied 20 ~ 200 mW/cm$^2$ with exposure time of typically 30 ~ 120 s. All the holographic gratings were carried out at room temperature.

## Morphology

Morphology of the composite film was studied with polarized optical microscopy (POM) and scanning electron microscopy (SEM, Hitachi S-4200). To visualize the grating formation with POM taken from the cell surface, cell was slightly inclined from the vertical position during horizontal irradiation of laser. For SEM observation at large magnification, laser grated films were fractured in liquid $N_2$, followed by extraction of LC with methanol for 24 hrs, and sputtering with gold before viewing under SEM.

## UV-visible Absorption

The reflection of specific wavelength by composite film was analyzed using an UV-visible spectrometer (Perkin Elmer, Lambda 20). Relative reflection efficiency was estimated from the peak intensity of the spectra.

## RESULT AND DISCUSSION

### Morphologies

Typical POM image of our gratings are shown in Figure 3 where the formation of grating is clearly seen.

Typical SEM images of grating formation is shown across the thickness of a composite film (Fig. 4). At medium magnification ( × 30,000), edge view of the film reveals alternatively stacked layers of LC-rich one (dark area) and polymer-rich one (bright area). High magnification ( × 80,000), taken on sample where LC was extracted in methanol, shows the spherical LC domains, order of some tens of nanometer in diameter, are lined up in the lamella plane [31].

As mentioned earlier, most significant difference between the HPDLC and conventional PDLC is the domain size of LC. In conventional PDLC, micron-sized LC domains ensure light scatterings at off state. On the other hand the domain size in HPDLC is order of nanometers which do not scatter lights of visible wavelength significantly. Smaller LC domains were obtained due to the high average functionality of monomer mixture, *viz.*, $4.2 \sim 4.8$ which is significantly higher than the conventional PDLC where the average functionality of monomer mixture is below 3. With monomers of high functionality, network forming reactions occur in such a rate that LC-polymer phase separation and coalescence of the small LC droplets into larger ones can not occur at a rate comparable to the rate of network formation. This keeps the LC domains in nanometer order.

Consequently, working mechanism with light should basically be different depending on the size of LC domains. In conventional PDLC over 80% of

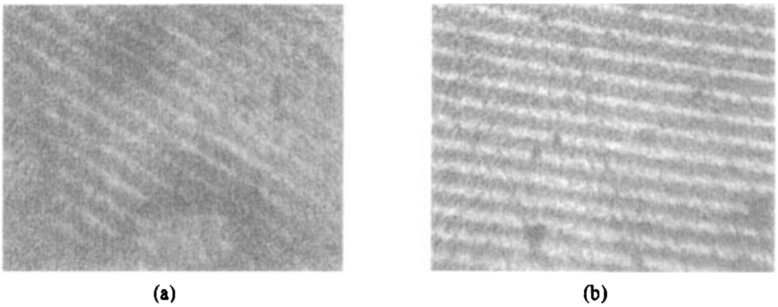

FIGURE 3 POM micrographs of HPDLC *vs.* monomer composition: (a) DPHPA/NVP = 4/1 and (b) DPHPA/NVP = 5.5/1. (See Color Plate XI).

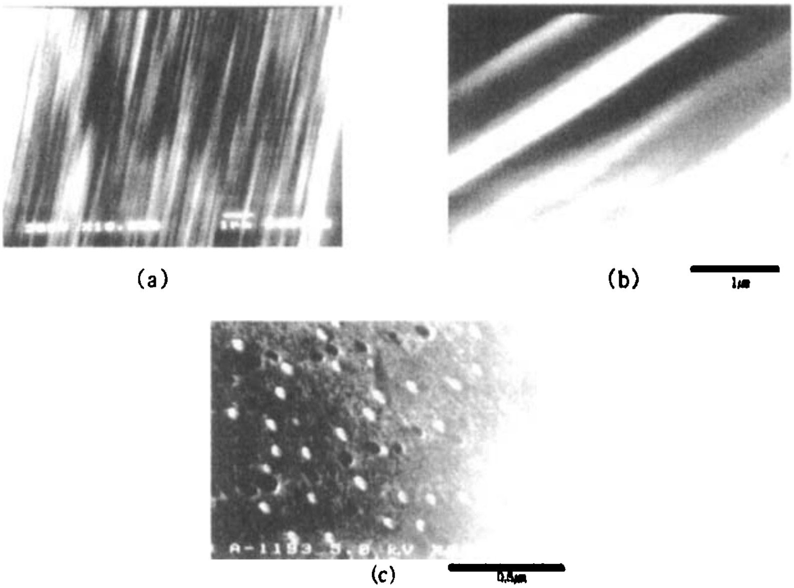

FIGURE 4 SEM morphology of HPDLC: a( × 10,000), b( × 30,000), c( × 80,000) (LC/monomer = 35/75, $I_o$ = 100 mW/cm$^2$).

the incident light is scattered, mostly in forward direction, and only about 10% are reflected. However, with HPDLC of the present mode reflection is dominant mechanism and scatterings should be negligible.

Figure 5 shows the UV-visible spectra of the composite films having various monomer ratios which were irradiated at various laser powers. Two peaks are found at about 480 and 580 nm, each corresponding to the reflection by holographic grating and absorption by dye rose bengal. The Bragg spacing is a bit smaller than the incident laser wave length (488 nm), due presumably to the shrinkage of mixture volume upon polymerization. As mentioned above, 480 nm peak will be approximated as reflection by gratings since scatterings are small with nanometer sized domains. It is noted that the 480 nm peak is much shaper than the 580 nm one and it becomes more intensive as the average functionality of monomer mixture increases. The intensification of 480 nm peak seems related to the low irradiation laser power to be discussed later.

With the increase in laser intensity, the intensity of 480 nm peak corresponding to holographic grating becomes much stronger as compared with 580 nm peak of rose bengal. This is especially true with lower monomer ratio. The peak intensity of higher monomer ratio is greater than the lower one especially at lower irradiation power, and it also generally increases with

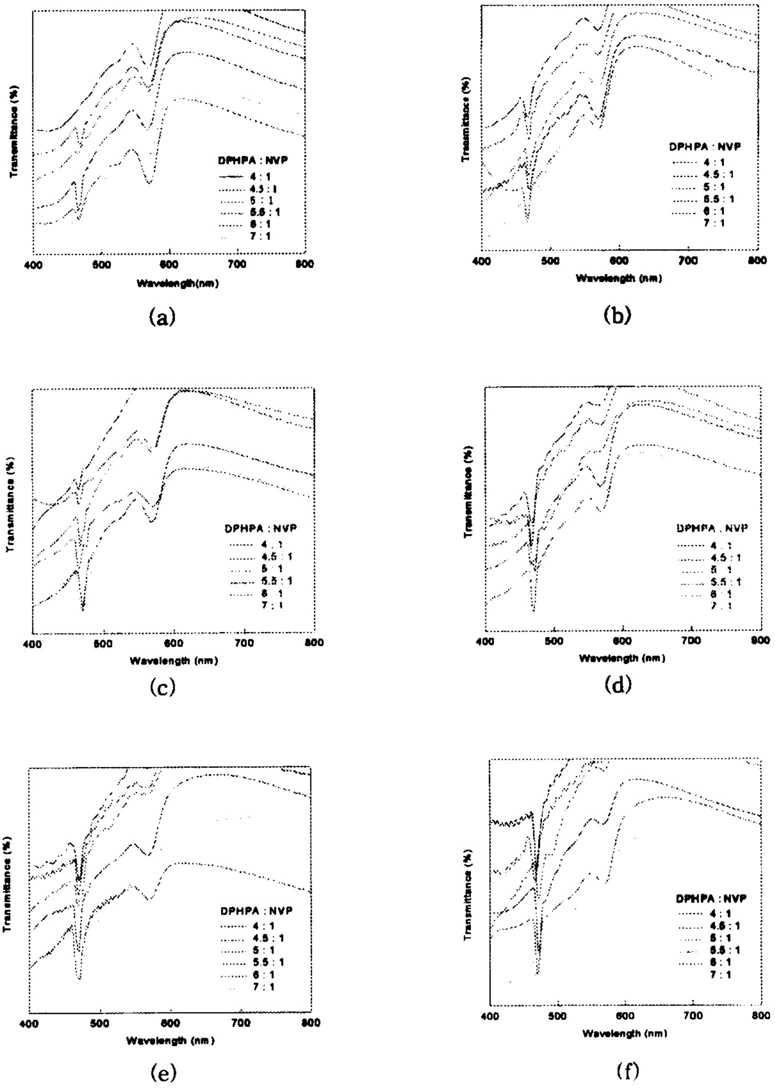

(a) (b) (c) (d) (e) (f)

FIGURE 5 Monomer ratio dependent UV-visible spectra of HPDLC films irradiated at; (a) 20 mW/cm$^2$, (b) 50 mW/cm$^2$, (c) 100 mW/cm$^2$, (d) 150 mW/cm$^2$, (e) 175 mW/cm$^2$, and (f) 200 mW/cm$^2$. (See Color Plate XII).

the increase in irradiation power. However, the effect of increasing irradiation power on peak intensity is more pronounced with lower monomer ratio.

In HPDLC the peak intensity should depend on the perfectness of holographic gratings. Obviously, more perfect gratings give higher peak intensity. Then, what governs the perfectness of grating? The answer should be the proper LC-polymer phase separation. Phase separation in polymerizing system is regarded as a liquid – liquid demixing process where spinodal decomposition prevails [32, 33]. Elementary Flory-Huggins theory is often used to obtain the interaction energy which is progressively increased with the progress of polymerization reaction.

Following Tanaka *et al.* [26], small and high density LC droplets gives higher reflection efficiency. Our results indicate that there may exist an optimum extent of LC-polymer phase separation according to the reaction kinetics of photoinitiated radical polymerization described earlier. It has been noted that $R_p$ as well as $R_i$ increases with irradiation intensity ($I_o$), although the effect on $R_i$ is more pronounced. $R_p$ also increases linearly with monomer concentration, which is proportional to the monomer ratio unless their reactivity is significantly different. So, high monomer ratio directly gives high reaction rate and hence augments crosslinking density of host polymers.

So, polymerization rate is by far the fastest when the highest monomer ratio is irradiated at the highest laser intensity, and it is by far the lowest when the lowest monomer ratio is irradiated at the lowest laser intensity. When the polymerization rate is too fast, rate of phase separations can not follow the rate of network formation and LC domains remain too small leading to imperfect gratings. Alternatively, coalescence of LC domains into larger ones become less plausible with highly viscous host polymer matrix, and this also retards phase separations. On the other hand, when the polymerization rate is too slow, phase separation can not take place in laboratory time scale due to the insignificant increase in $G_{\text{mix}}$. Therefore, there should exist an optimum monomer ratio for the desired maximum reflection depending on the irradiation intensity.

Reflection efficiency-irradiation power relationships are collected in Figure 6 which shows monotonic increase of reflection efficiency with irradiation power for low monomer ratio (DPHPA/NVP = 5.5), and maximum for high monomer ratio (DPHPA/NVP = 6). The power intensity of maximum reflection efficiency becomes lower as the monomer ratio increases.

Same data were replotted for reflection efficiency-monomer ratio in Figure 7 which shows monotonic increase at low, asymptotic increase at medium, and monotonic decrease at high laser power as well. This may imply that reflection efficiency is more sensitive to the monomer ratio as compared with irradiation power, which could be inferred from Eq. (4). That is, $R_p$ is directly proportional to the monomer concentration, and square root of irradiation power.

Reflection efficiency-monomer ratio-irradiation intensity relationships are plotted in three dimensional form in Figure 8. From this plot, it is visualized

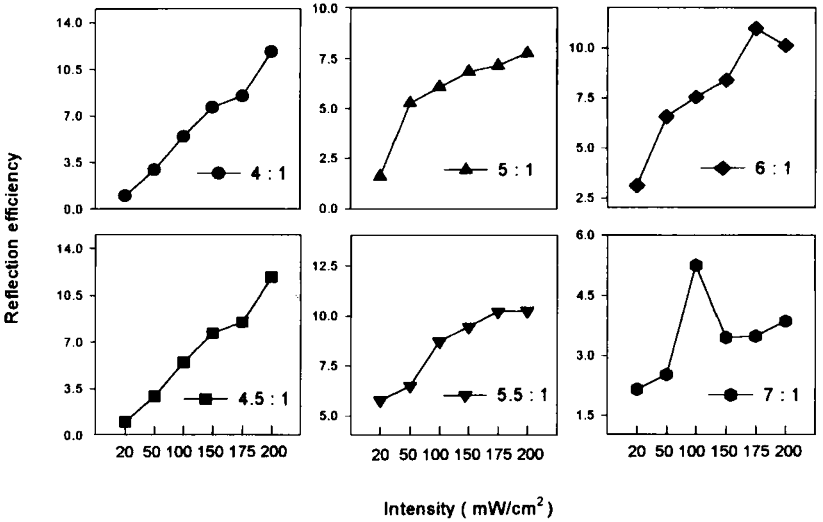

FIGURE 6 Reflection efficiency *vs.* laser intensity of HPDLC films prepared with various monomer ratios (DPHPA/NVP).

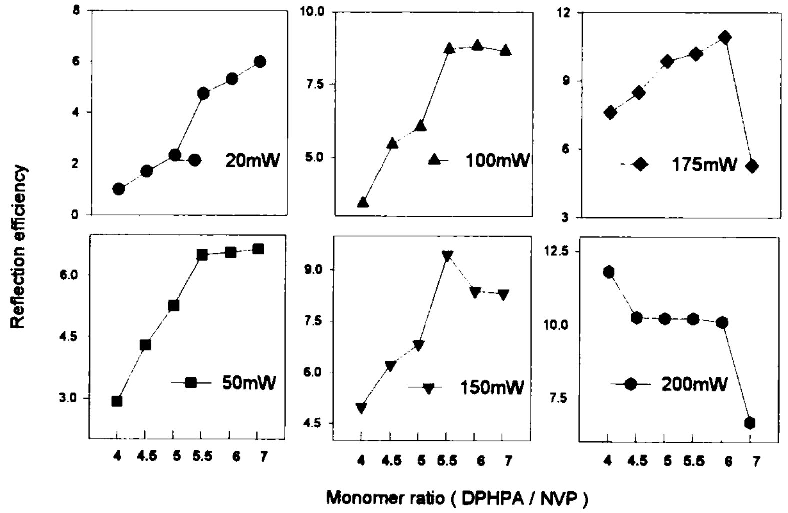

FIGURE 7 Reflection efficiency *vs.* monomer ratio of HPDLC films irradiated at various laser intensities.

that contour for maximum reflection generally follows the diagonal connecting the two points (highest monomer ratio, lowest irradiation power) and (lowest monomer ratio, highest irradiation power). This implies

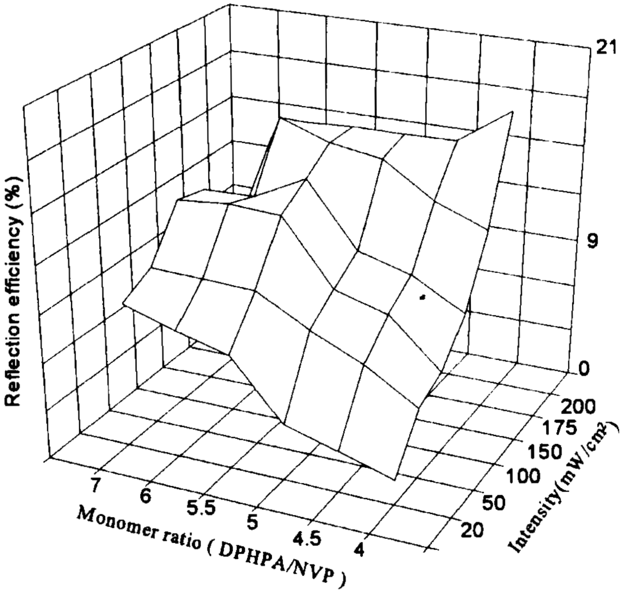

FIGURE 8 Reflection efficiency-monomer ratio-laser intensity relationships of HPDLC films (LC/monomer = 35/65).

that polymerization rate should be neither too high nor too low to augment the reflection efficiency. Only at controllable polymerization rate, rate of phase separation is comparable with rate of polymerization and hence the domain size is appropriately small and its density is high enough to reflect maximum. At the other two extremes, *i.e.*, when both the monomer composition and irradiation intensity are too high or too low, phase separation is too small due to the extremely fast and slow polymerization rates and appropriate phase separations do not occur.

## Acknowledgment

The research is in the program of G7 project which has been supported by the Korea Ministry of Commerce, Industry and Energy, and Ministry of Science and Technology. The financial support is gratefully acknowledged.

## References

[1] S. Zumer and J. W. Doane, *Phys. Rev. A*, p. 3373 (1986).
[2] P. S. Drzaic and A. M. Gonzales, *Appl. Phys. Lett.*, **73**, 1332 (1993).
[3] J. L. Fergason, SID Technical Digest, **16**, 68 (1985).

[4] G. P. Montgomery, *Proc. SPIE*, **242**(9), 1080 (1989).
[5] Y. Miyamoto, H. Kikuchi, Y. Morimura and T. Kajiyama, *New Polym. Mater.*, **2**, 1 (1990).
[6] J. W. Doane, In: *Liquid Crystal-Applications and Usage*, Vol. 1, World Scientific, Jersey, 1990.
[7] G. P. Crawford, J. W. Doane and S. Zumer, In: *Handbook of Liquid Crystal Research*, P. J. Collings and J. S. Patel (Eds.), Oxford University Press, Oxford, 1997.
[8] P. Drzaic, *Mol. Cryst. Liq. Cryst.*, **154**, 289 (1988).
[9] H. S. Kitzerow, *Liquid Crystals*, **16**(1), 1 (1994).
[10] J. L. West, *Mol. Cryst. Liq. Cryst.*, **157**, 427 (1988).
[11] P. S. Drzaic, *Liquid Crystal Dispersion*, World Scientific Singapore, 1995.
[12] B. K. Kim and Y. S. Ok, *J. Polym. Sci., Polym. Phys.*, **32**, 561 (1994).
[13] B. K. Kim and S. H. Kim, *J. Polym. Sci., Polym. Phys.*, **36**, 55 (1998).
[14] B. K. Kim, Y. S. Ok and C. H. Choi, *J. Polym. Sci., Polym. Phys.*, **33**, 707 (1995).
[15] B. K. Kim, S. H. Kim and C. H. Choi, *Mol. Cryst. Liq. Cryst.*, **261**, 605 (1995).
[16] P. Nolan, M. Tillin and D. Coates, *Mol. Cryst. Liq. Cryst. Letters*, **8**(6), 129 (1992).
[17] T. Fujisawa, H. Ogawa and K. Muruyama, *Jpn. Display*, p. 690 (1989).
[18] H. Ono and N. Kawatsuki, *Jpn. J. Appl. Phys.*, Part 1, **33**, 6268 (1994).
[19] G. Smith, *Mol. Cryst. Liq. Cryst.*, **180**, 201 (1990).
[20] Y. H. Cho and B. K. Kim, *J. Polym. Sci., Polym. Phys.*, **36**, 1393 (1998).
[21] T. J. Bunning, L. V. Natarajan, V. P. Tondiglia, G. Dougherty and R. L. Sutherland, *J. Polym. Sci., Polym. Phys.*, **35**, 2825 (1997).
[22] R. L. Sutherland, V. P. Tondiglia, L. V. Natarajan, T. J. Bunning and W. W. Adams, *Appl. Phys. Lett.*, **64**, 1074 (1994).
[23] J. Zhang, C. R. Carlen, S. Palmer and M. B. Sponsler, *J. Amer. Chem. Soc.*, **116**, 7055 (1994).
[24] M. E. C. Rosa, V. P. Tondiglia and L. V. Natarajan, *J. Appl. Polym. Sci.*, **68**, 523 (1998).
[25] H. Murai, T. Gotoh, M. Suzuki, E. Hasegawa and K. Mizoguchi, SPIE, Vol. 1665, 230 (1992).
[26] K. Tanaka, K. Kato, M. Date and S. Sakai, *SID 95 DIGEST*, p. 267 (1995).
[27] M. Date, N. Naito, K. Tanaka, K. Kato and S. Sakai, Asia Display, **95**, 603 (1995).
[28] G. Odian, "*Principles of Polymerization*", 2nd edn., Wiley, New York, 1981.
[29] R. R. B. Seymour and C. E. Carraher, "*Polymer Chemistry*", 2nd edn., Marcel Dekker, New York, 1988.
[30] B. K. Kim, E. Y. Hong and Y. S. Ok, *Korea Polym. J.*, **5**(2), 77 (1997).
[31] T. J. Bunning, L. V. Natarajan, V. P. Tondiglia, G. Dougherty, R. L. Sutherland, D. L. Vezie, and W. W. Adams, *Polymer Communications*, **37**, 3147 (1996).
[32] J. C. Lin and P. L. Taylor, *Mol. Cryst. Liq. Cryst.*, **237**, 25 (1993).
[33] J. Y. Kim and P. Palffy-Muhoray, *Mol. Cryst. Liq. Cryst.*, **203**, 93 (1991).